



Ionic liquid-immobilized hybrid nanomaterial: an efficient catalyst in the synthesis of benzimidazoles and benzothiazoles via anomeric-based oxidation

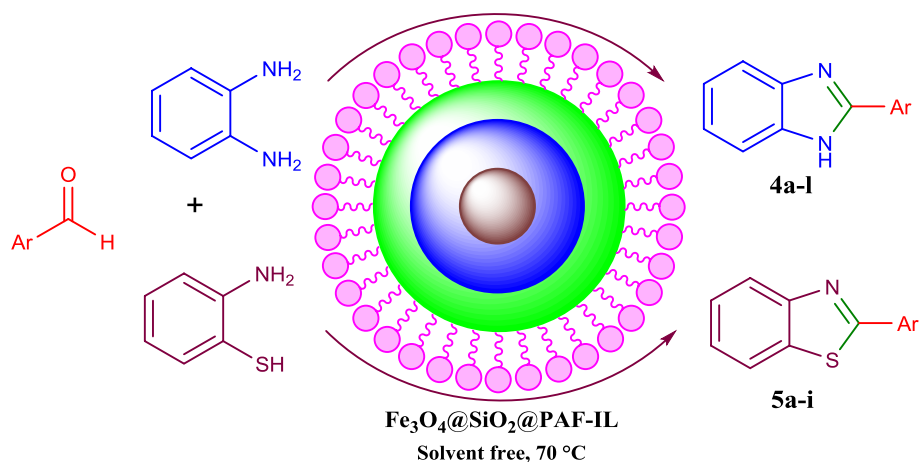
Mohammad Ali Bodaghifard^{1,2} · Saeideh Shafi¹

Received: 8 April 2020 / Accepted: 1 September 2020
© Iranian Chemical Society 2020

Abstract

In this study, a novel ionic liquid immobilized on silica-coated cobalt-ferrite magnetic nanoparticles. This novel hybrid nanostructure ($\text{CoFe}_2\text{O}_4@ \text{SiO}_2@ \text{PAF-IL}$) was characterized by various microscopic and spectroscopic techniques including Fourier transformation infrared spectroscopy (FT-IR), X-ray powder diffraction (XRD), field emission scanning electron microscopy (SEM), the electron-dispersive X-ray spectroscopy (EDS), vibrating sample magnetometer (VSM), and thermogravimetric analysis (TGA/DTG). The catalytic activity of prepared nanomaterial was considered in the synthesis of the benzothiazole and benzimidazole derivatives. This method has several advantages such as good to excellent yields, short reaction times, solvent-free and environmentally-benign conditions, and simple work-up. Besides, nanocatalyst can be easily separated from the reaction mixture with the external magnetic field and reused several times without any loss of its catalytic activity.

Graphic abstract



Keywords Benzimidazoles · Benzothiazoles · Heterogeneous catalysis · Hybrid nanostructure · Magnetic nanoparticles

✉ Mohammad Ali Bodaghifard
m-bodaghifard@araku.ac.ir

¹ Department of Chemistry, Faculty of Science, Arak University, 38156-88138 Arak, Iran

² Institute of Nanosciences and Nanotechnology, Arak University, 38156-88138 Arak, Iran

Introduction

From the initial use of ionic liquids (ILs), which are made up of cationic and anionic components, they have found applications in various fields such as environmentally friendly solvents and catalysis because they have the specific features such as undetectable vapor pressure, good thermal stability,

and high solubility [1–5]. Ionic liquids have successfully been used in various catalytic areas affording high catalytic performance [2–5]. Unfortunately, the difficulties in the recovery and unendurable viscosity of ILs have restrained their wide applications in catalytic reactions [2–5]. So, the heterogenization of ILs on appropriate porous carriers or suitable magnetic nanoparticles would be a viable and appealing approach to fabricate the efficient solid catalyst with superior activity and stability [6–9]. Furthermore, the heterogenized ILs on magnetic nanoparticles have found wonderful applications such as adsorbent for magnetic solid-phase extraction (SPE) of sulfonylurea herbicides, adsorbent for magnetic dispersive SPE of Cephalosporins, and removal of anionic dye from water [10–12].

The magnetic nanoparticles (MNPs) not only have high surface areas but also they can be easily separated by using an external magnetic field and do not have tedious separation procedures which resulted from the small sizes of nanoparticles and have other advantages including easy synthesis, easy surface modification and functionalization, low toxicity, and low cost [13–15]. Magnetic nanoparticles have many important applications such as drug delivery [16, 17], food industry [18], agriculture [19], textile industry [20], water treatment [21], and catalysis [6–9]. However, magnetic nanoparticles can easily aggregate into larger clusters because of their anisotropic dipolar attraction. Besides, they have other deficiencies such as leaching under acidic conditions and being susceptible to auto-oxidation and toxicity. Therefore, it is necessary to protect the surface of MNPs to reduce these undesirable features. For this purpose, MNPs are usually coated with a polymeric or inorganic matrix [6–9]. Among inorganic compounds, SiO_2 can be a suitable candidate for protecting the surface of MNPs due to its high chemical and thermal stability and most importantly its easy modification by a wide range of functional groups, which increase the chemical and colloidal stability of these compounds [6–9]. The cobalt-ferrite nanoparticles (CoFe_2O_4 NPs) have appealed much attention due to their high chemical stability, thermal and corrosive stability, and moderate saturation magnetization [22–24, 38].

Green or sustainable chemistry is the designing of chemical processes with the reduction or elimination of harmful substances. Each green reaction should have three components: solvent, reagent or catalyst, and energy consumption. In recent years, a wide spectrum of the organic syntheses is designed to reduce byproduct or waste generation, reduce the use of hazardous reagents and solvents, and improve energy efficiency [25, 26].

Benzimidazoles and benzothiazoles are bicyclic heterocyclic compounds containing imidazole and thiazole scaffold with great properties [27]. They have biological activity such as anti-inflammatory [28], antimicrobial [29] anticancer [30], antiviral [31], antihypertensive [32], and

anticonvulsant activity [33]. Therefore, these compounds are attractive targets for synthesis. There are different methods for the synthesis of benzimidazoles and benzothiazoles that involve multistep synthesis, use of toxic reagents and solvent, long reaction times, and low yields. Therefore, several modified processes have been reported in the literature using different catalysts such as Fe(III)-Schiff base/SBA-15 [34], $[\text{Dsim}]\text{Cl}/\text{FeCl}_3$ [35], hybrid crystal $\text{NH}_3(\text{CH}_2)_4\text{NH}_3\text{SiF}_6$ [36], $\text{NiFe}_{2-x}\text{Eu}_x\text{O}_4$ nanostructures [37], Co-doped NiFe_2O_4 [38], 1,4-Diazabicyclo [2.2.2] octanium diacetate [39], and $\text{NH}_3(\text{CH}_2)_5\text{NH}_3\text{BiCl}_5$ [40].

As part of our continuous effort to develop efficient heterogeneous magnetic nanocatalysts and green organic reactions [3a, 41–48], herein we have reported the preparation of a novel heterogeneous ionic liquid-supported hybrid nanostructure ($\text{CoFe}_2\text{O}_4@\text{SiO}_2@\text{PAF-IL}$) as an impressive catalyst for the synthesis of benzimidazole, benzothiazole derivatives (Scheme 2). The presented method has considerable efficiency of the catalyst and environmental compatibility. Also, the catalyst was inexpensive and highly efficient, and it could easily be recovered and reused.

Experimental

All reagents were purchased from reputable chemical companies (Merck, Across, Fluka) and were used without further purification. Melting points were measured by using electrothermal digital apparatus and are uncorrected. Obtained products were identified with a comparison of their melting points and spectral data reported in the literature. The FT-IR spectra were recorded by Unicom Galaxy Series. The ^1H , ^{13}C NMR spectra for obtained products were reported on Bruker DRX-300 spectrometer operating at 300 and 75 MHz, respectively, in $\text{DMSO}-d_6$ with TMS as an internal standard. The crystal structure was carried out by Philips Xpert X-ray powder diffraction (XRD) diffractometer ($\text{Cu-K}\alpha$ radiation and $\lambda = 0.15406$) in the range of Bragg angle 10–80 using 0.05° as the step length. The thermal stability of $\text{CoFe}_2\text{O}_4@\text{SiO}_2@\text{PAF-IL}$ was investigated by a thermogravimetric analyzer with a model Mettler TA4000 System under an N_2 atmosphere at a heating rate of $10^\circ\text{C min}^{-1}$. The surface morphology and elemental content of $\text{CoFe}_2\text{O}_4@\text{SiO}_2@\text{PAF-IL}$ were investigated on a Hitachi S-4160. The elemental chemical analysis [energy-dispersive X-ray spectroscopy (EDS)] coupled with SEM was reported for the characterization of chemical elements of the $\text{CoFe}_2\text{O}_4@\text{SiO}_2@\text{PAF-IL}$ catalyst. The magnetization and hysteresis loop for the synthesized magnetic nanoparticles were measured at room temperature using a 7300 VSM system with a maximum field of 10 kOe.

Preparation of the cobalt ferrite nanoparticles (CoFe₂O₄)

Magnetic cobalt ferrite nanoparticles were prepared by the co-preparation method according to the procedure reported in the literature [49]. Firstly, COCl₂•6H₂O (5 mmol, 1.8 g), FeCl₃•6H₂O (10 mmol, 2.7 g) were added to 50 mL of deionized water in a round bottom flask (100 mL), and the mixture was stirred at room temperature for 10 min. The pH was adjusted to 11–12 using NaOH (0.3 M) solution. The reaction mixture was stirred at 80 °C for 1 h. After cooling to room temperature, the precipitate was separated off using a magnet and washed with deionized water several times and finally washed with ethanol and dried in an oven at 80 °C.

Synthesis of silica-coated MNPs (CoFe₂O₄@SiO₂)

The silica shell was coated onto CoFe₂O₄ nanoparticles via hydrolysis of TEOS in basic solution [45]. Magnetic cobalt ferrite nanoparticles (1 g), ethanol (40 mL), deionized water (6 mL), and ammonia 25% (1.5 mL) were introduced in a 100-mL flask and sonicated for 20 min. Then, Tetraethyl-orthosilicate (TEOS) (1.4 mL) was added to the mixture. The reaction mixture was stirred at room temperature for 12 h. Finally, the precipitate was separated by a magnet and washed with deionized water several times and ethanol and dried in an oven at 80 °C.

Synthesis of 3-aminopropyl-functionalized magnetic nanoparticles (CoFe₂O₄@SiO₂-PrNH₂)

CoFe₂O₄@SiO₂-PrNH₂ nanoparticles were synthesized using a reported procedure [47]. CoFe₂O₄@SiO₂ nanoparticles (1 g) were dispersed in 50 ml toluene for 10 min under sonication. Then, (3-aminopropyl)triethoxysilane (APTES) (2 g) was added and refluxed for 24 h at 110 °C. Finally, the precipitate was separated using a magnet and washed with toluene several times and dried in an oven at 80 °C.

Preparation of poly(aniline-formaldehyde) silica-coated MNPs (CoFe₂O₄@SiO₂@PAF)

To synthesize the CoFe₂O₄@SiO₂@PAF nanocomposite, a mixture of aniline (0.5 g), formaldehyde (1 g), and CoFe₂O₄@SiO₂-PrNH₂ (1 g) in 25 mL DMF at 100 ml round-bottomed flask was stirred under sonication. Then, the mixture was stirred with a magnetic stirrer for 48 h at 100 °C. After the reaction was completed, the precipitate was washed several times with hot ethanol and dried in an oven at 80 °C.

Stabilization of ionic liquid on magnetic nanoparticles (CoFe₂O₄@SiO₂@PAF-IL)

To prepare the CoFe₂O₄@SiO₂@PAF-IL hybrid nanostructure, CoFe₂O₄@SiO₂@PAF (1 g) was mixed with K₂CO₃ (0.5 g) and MeI (2 mL) in DMF (25 mL) under sonication for 10 min. The resulted mixture was stirred at 100 °C for 24 h. Finally, the precipitate was separated using a magnet and washed with deionized water several times and dried in an oven at 80 °C.

General procedure for the synthesis of benzimidazole and benzothiazole derivatives

CoFe₂O₄@SiO₂@PAF-IL (20 mg) was added to the mixture of aromatic aldehyde (1 mmol), o-phenylenediamine (1 mmol, 0.11 g), or 2-aminobenzenethiol (1 mmol, 0.125 g) and heated in solvent-free conditions at 70 °C for an appropriate time. After completion, the resulting mixture was diluted with hot ethanol (10 mL), and the catalyst was easily separated using an external magnet. Finally, the gained precipitate was recrystallized in ethanol to afford the pure product.

Selected spectroscopic data

2-(p-tolyl)-1H-benzo[d]imidazole (4b): IR (KBr, ν_{\max}): 3342, 3257, 3035, 2948, 2871, 1678, 1652, 1580, 1523, 1335, 832 cm⁻¹. ¹H NMR (300 MHz, DMSO-*d*₆): 12.25 (1H, s, NH), 7.15–8.05 (8H, m, H_{Ar}), 2.19 (3H, s, CH₃) ppm. Anal. Calcd. for C₁₄H₁₂N₂: C, 80.74; H, 5.81; N, 13.45. Found: C, 80.67; H, 5.79; N, 13.59.

4-(1H-benzo[d]imidazol-2-yl)-2-methoxyphenol (4k): IR (KBr, ν_{\max}): 3338, 3059, 2935, 2841, 1602, 1578, 1506, 1273, 1031 cm⁻¹. ¹H NMR (300 MHz, DMSO-*d*₆): δ = 12.45 (1H, s, NH), 9.35 (1H, s, OH), 6.17–7.55 (7H, m, H_{Ar}), 3.44 (3H, s, CH₃) ppm. Anal. Calcd. for C₁₄H₁₂N₂O₂: C, 69.99; H, 5.03; N, 11.66. Found: C, 67.11; H, 5.09; N, 11.76.

4-(1H-benzo[d]imidazol-2-yl)-N,N-dimethylaniline (4l): IR (KBr, ν_{\max}): 3338, 3020, 2918, 2800, 1608, 1500, 1470, 1250, 837, 746 cm⁻¹. ¹H NMR (300 MHz, DMSO-*d*₆): δ = 6.35–7.79 (8H, m, H_{Ar}), 3.16 (6H, s, 2CH₃) ppm. Anal. Calcd. for C₁₅H₁₅N₃: C, 75.92; H, 6.37; N, 17.71. Found: C, 75.81; H, 6.45; N, 17.83.

2-(4-methoxyphenyl)benzo[d]thiazole (5c): IR (KBr, ν_{\max}): 3380, 3057, 2995, 1602, 1578, 1500, 1257, 1028 cm⁻¹. ¹H NMR (300 MHz, DMSO-*d*₆): δ = 6.91–7.92 (8H, m, H_{Ar}), 3.66 (3H, s, CH₃) ppm. Anal. Calcd. for C₁₄H₁₁NOS: C, 69.68; H, 4.59; N, 5.80; S, 13.29. Found: C, 69.51; H, 4.67; N, 5.69; S, 13.41.

4-(benzo[d]thiazol-2-yl)-N,N-dimethylaniline (5i): IR (KBr, ν_{\max}): 3382, 3053, 2963, 2899, 1608, 1500, 1367, 1188, 817, 752 cm⁻¹. ¹H NMR (300 MHz, DMSO-*d*₆):

$\delta = 6.62\text{--}7.85$ (8H, m, H_{Ar}), 3.14 (6H, s, $2CH_3$) ppm. Anal. Calcd. for $C_{15}H_{14}N_2S$: C, 70.83; H, 5.55; N, 11.01; S, 12.60. Found: C, 70.69; H, 5.63; N, 10.97; S, 12.73.

Result and discussion

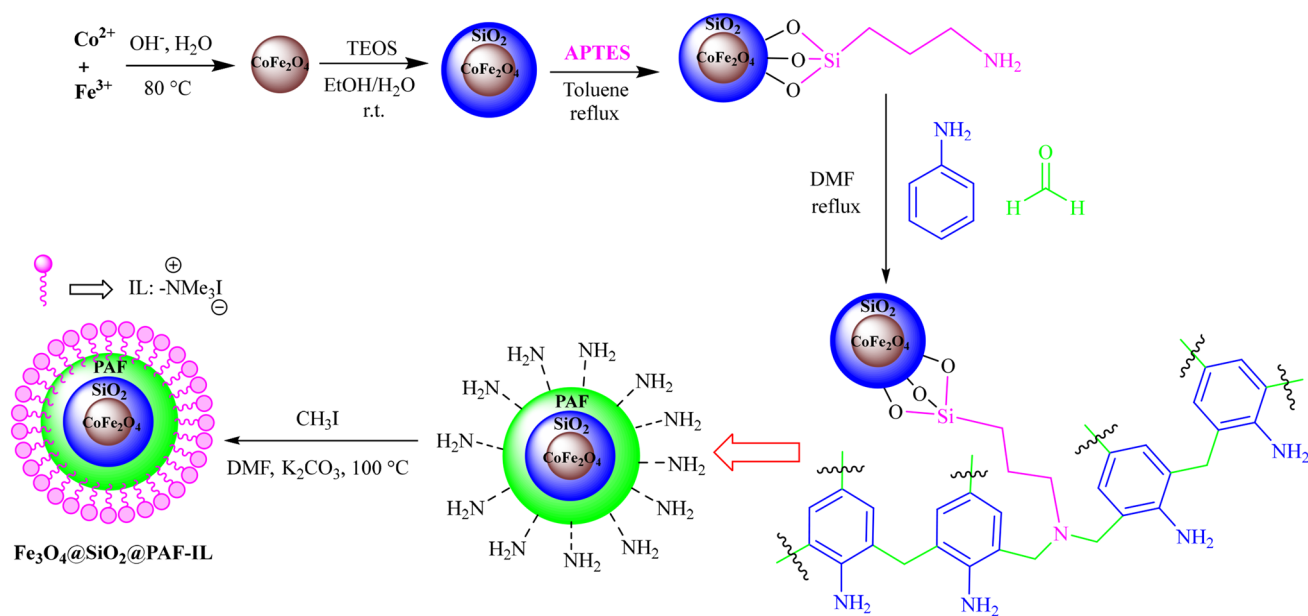
Preparation and characterization of the hybrid nanostructure

The magnetic hybrid nanoparticles were prepared sequentially, as illustrated in scheme 1. Firstly, $CoFe_2O_4$ was prepared easily by the co-preparation method from the chemical reaction of Co^{2+} and Fe^{3+} ions in the base conditions [49]. Then, $CoFe_2O_4$ nanoparticles were coated with a silica layer using the stöber method [45]. The aminopropyl-modified silica-coated $CoFe_2O_4$ nanoparticles were prepared by the reaction of $CoFe_2O_4@SiO_2$ with (3-aminopropyl)triethoxysilane (APTES) which can bind covalently to the free-OH groups at the surface of the particles and afforded the $CoFe_2O_4@SiO_2\text{-PrNH}_2$. The reaction of formaldehyde and aniline with $CoFe_2O_4@SiO_2\text{-PrNH}_2$ nanoparticles resulted in the construction of $CoFe_2O_4@SiO_2\text{-PAF}$ nanocomposite [50]. Finally, the hybrid nanomaterial $CoFe_2O_4@SiO_2\text{-PAF-IL}$ was fabricated by the reaction of excess methyl iodide with free amine groups on the surface of $CoFe_2O_4@SiO_2\text{-PAF}$ nanocomposite. The resulting precipitate was washed with ethanol and dried in the vacuum oven to gain the final hybrid nanomaterial ($CoFe_2O_4@SiO_2\text{-PAF-IL}$). The Fourier transform infrared (FT-IR) spectroscopy, X-ray diffraction (XRD), field emission scanning electron microscopy

(FE-SEM), energy-dispersive X-ray spectroscopy (EDS), thermogravimetric analysis (TGA), and vibrating sample magnetometry (VSM) were employed to identify and characterize the prepared hybrid nanostructure.

The FT-IR spectra of $CoFe_2O_4$ (a), $CoFe_2O_4@SiO_2$ (b), $CoFe_2O_4@SiO_2\text{-Pr-NH}_2$ (c), $CoFe_2O_4@SiO_2\text{-PAF}$ (d) and $CoFe_2O_4@SiO_2\text{-PAF-IL}$ (e) are shown in Fig. 1. The FT-IR spectrum of magnetic $CoFe_2O_4$ nanoparticles shows the characteristic Fe-O and Co-O absorption bands around 590 and 390 cm^{-1} (Fig. 1a) [45]. Also, a broadband around 3450 cm^{-1} refers to the stretching vibration vibrations of H-O-H groups on the surface of nanoparticles. $CoFe_2O_4@SiO_2$ shows characteristic FT-IR bands at around 1089 cm^{-1} , 947 cm^{-1} , 860 cm^{-1} , and 457 cm^{-1} which are attributed to the asymmetric stretching, symmetric stretching, in-plane bending, and rocking mode of the Si-O-Si group, respectively, that confirms the formation of SiO_2 shell (Fig. 1b) [48]. The absorption band at 1640 cm^{-1} is referred to stretching vibration mode of Si-OH groups. The weak absorptions at 2920 and 2935 cm^{-1} are attributed to symmetric and asymmetric stretching modes of the attached alkyl groups (Fig. 1c-e) [47]. Thus, the results confirm that the functional groups were successfully grafted on the surface of $CoFe_2O_4$ nanoparticles.

The X-ray powder diffraction (XRD) patterns were used to study the crystallinity of prepared nanostructure. The XRD patterns of $CoFe_2O_4$ (a) and $CoFe_2O_4@SiO_2\text{-PAF-IL}$ (b) show characteristic peaks at 74.5, 62.8, 57.2, 53.9, 43.2, 35.6, and 30°, which can be attributed to the 533, 440, 511, 422, 400, 311, and 220 planes of $CoFe_2O_4$, respectively (Fig. 2a). These data are according to the standard $CoFe_2O_4$



Scheme 1 Schematic route for the synthesis of $CoFe_2O_4@SiO_2@PAF-IL$ hybrid nanostructure

Fig. 1 The FT-IR spectra of CoFe_2O_4 (a), $\text{CoFe}_2\text{O}_4@ \text{SiO}_2$ (b), $\text{CoFe}_2\text{O}_4@ \text{SiO}_2@ \text{Pr-NH}_2$ (c), $\text{CoFe}_2\text{O}_4@ \text{SiO}_2@ \text{PAF}$ (d), and $\text{CoFe}_2\text{O}_4@ \text{SiO}_2@ \text{PAF-IL}$ (e)

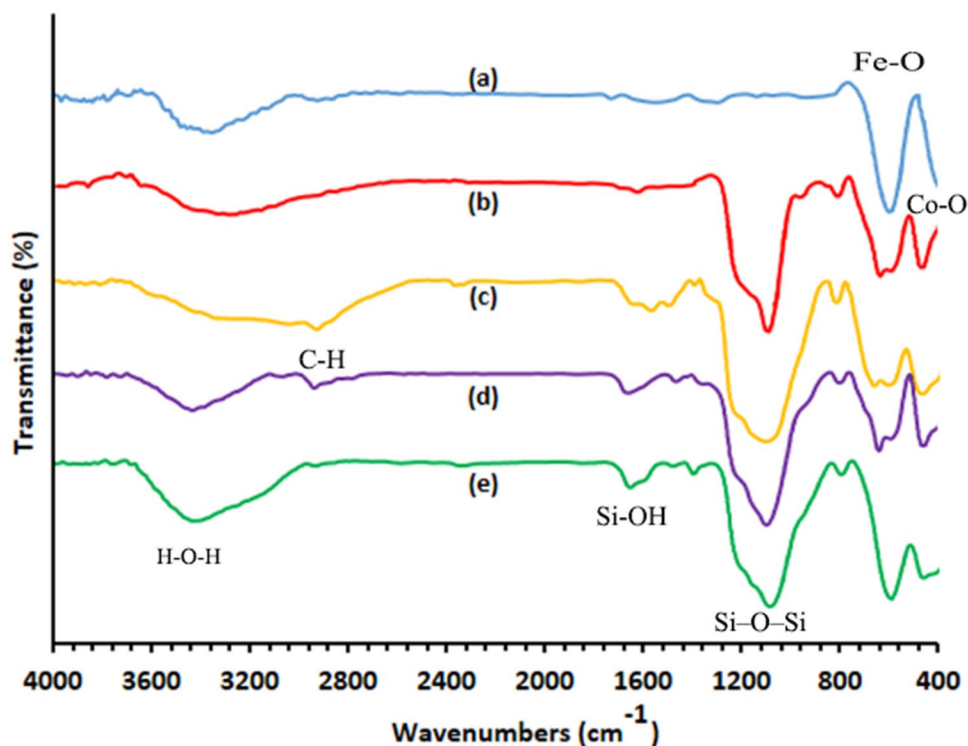
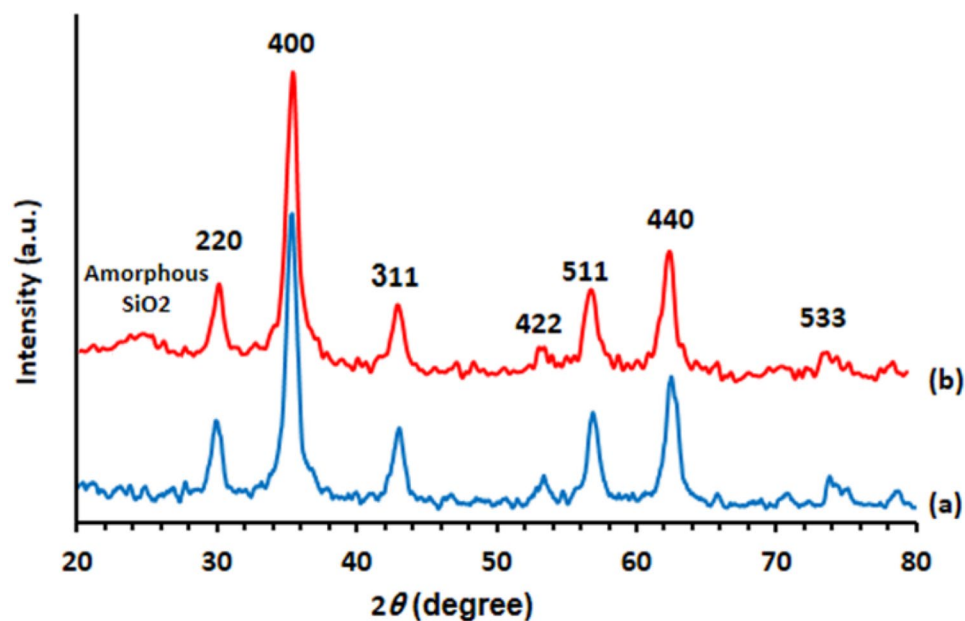


Fig. 2 XRD patterns of CoFe_2O_4 (a) and $\text{CoFe}_2\text{O}_4@ \text{SiO}_2@ \text{PAF-IL}$ (b)



sample (standard JCPDS no. 22-1086) and confirm a cubic spinel structure for CoFe_2O_4 nanoparticles. The broad peak at $2\theta = 23\text{--}28^\circ$ can be attributed to the amorphous SiO_2 coated on the surface of CoFe_2O_4 core in $\text{CoFe}_2\text{O}_4@ \text{SiO}_2@ \text{PAF-IL}$ nanostructure (Fig. 2b) [48]. The average crystallite sizes estimated using Scherrer's equation ($D = 0.9 \lambda / \beta \cos \theta$). The crystallite size of $\text{CoFe}_2\text{O}_4@ \text{SiO}_2@ \text{PAF-IL}$ calculated from the width of the peak at $2\theta = 35.6^\circ$ (311) is 20 nm,

which is in the range determined using FE-SEM analysis (Fig. 4a).

The thermal stability of $\text{CoFe}_2\text{O}_4@ \text{SiO}_2@ \text{PAF-IL}$ was determined by thermal analysis of TGA and DTG at $50\text{--}950^\circ \text{C}$ range (Fig. 3). The magnetic nanomaterial shows three weight loss steps, and the total weight loss of MNPs in three steps was estimated at 17 wt%. The first stage, including a low amount (2.5%) of weight loss at $T < 200^\circ \text{C}$,

Fig. 3 TGA and DTG of $\text{CoFe}_2\text{O}_4@SiO_2@PAF-IL$

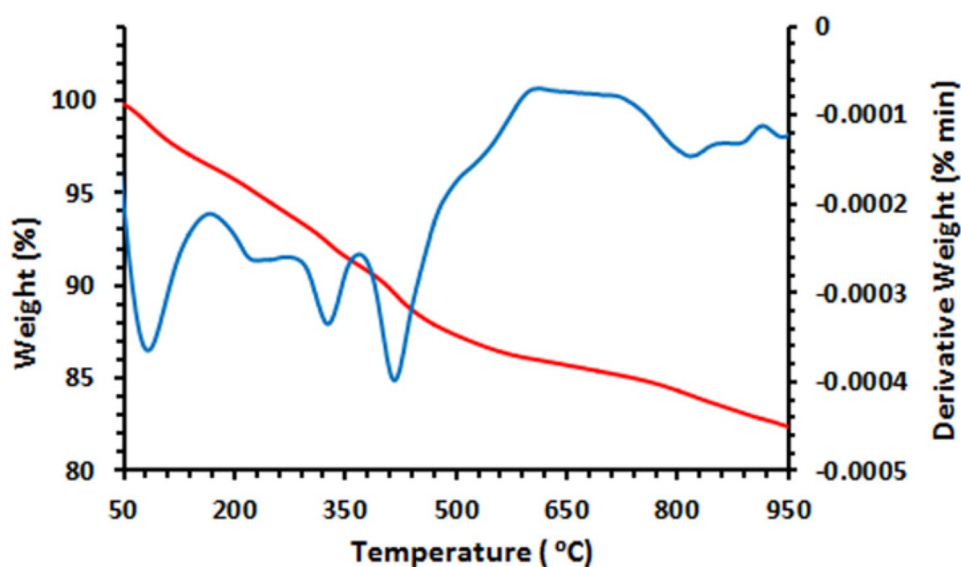
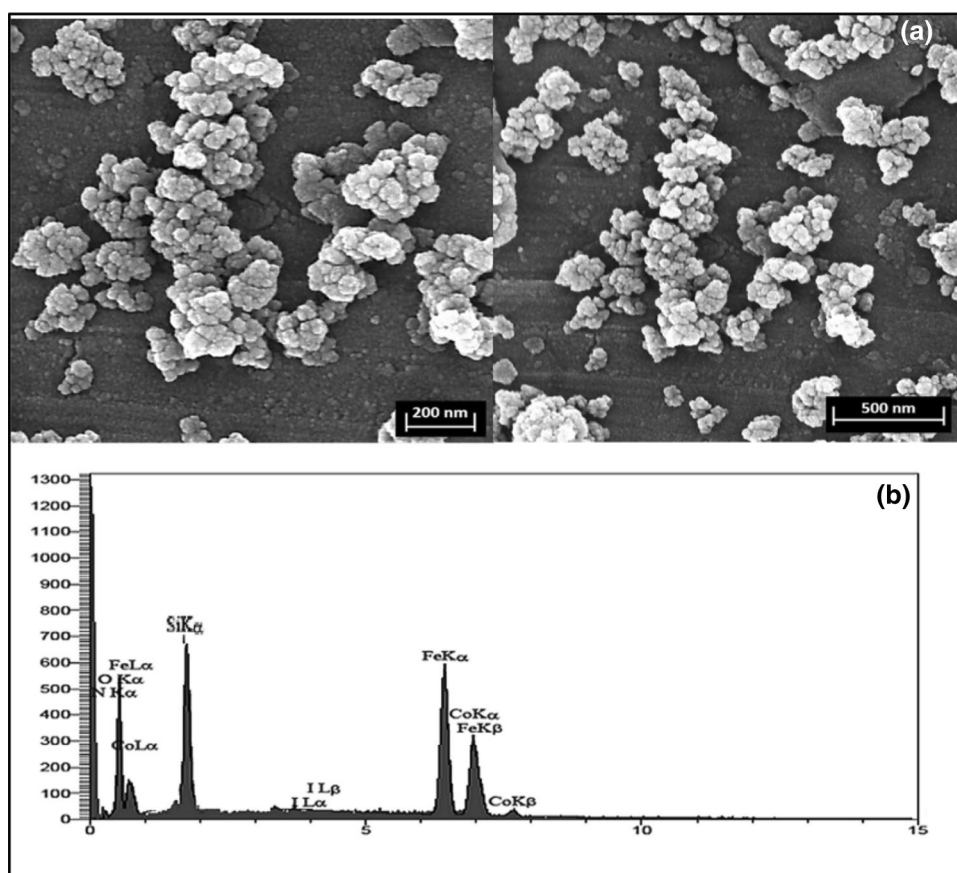


Fig. 4 FE-SEM image (a), and EDX analysis (b) of $\text{CoFe}_2\text{O}_4@SiO_2@PAF-IL$



was due to the removal of the physically adsorbed solvent, water, and surface hydroxyl groups. The second step at about 200 °C to nearly 580 °C is attributed to the decomposition of the organic layer in the nanocomposite. Therefore, the weight loss between 200 and 580 °C gives the organic moiety ratios grafted on the prepared nanomaterial. The organic

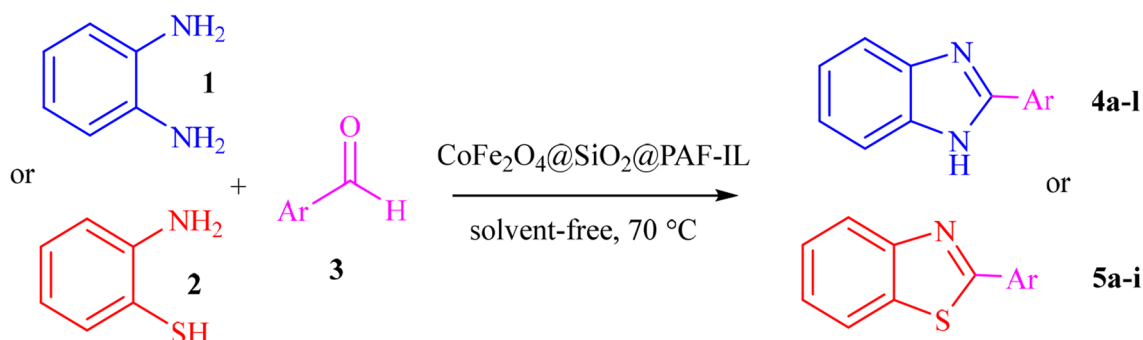
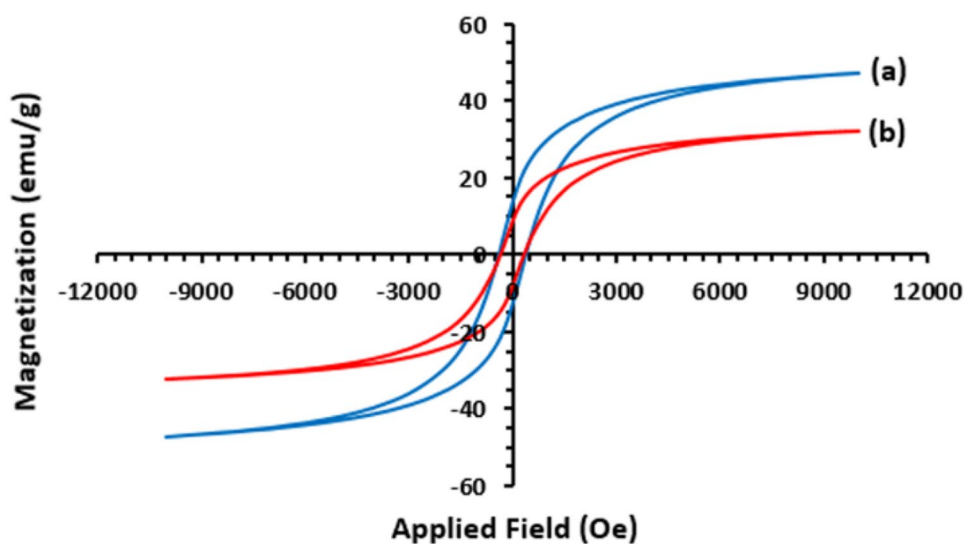
moiety grafted on the $\text{CoFe}_2\text{O}_4@SiO_2@PAF-IL$ was approximately 10% wt. The third step shows weight loss of 4.5% at $T > 580$ °C attributed to the destruction and deformation of the silica layer.

The size and morphology of the $\text{CoFe}_2\text{O}_4@SiO_2@PAF-IL$ particles were investigated by the field emission

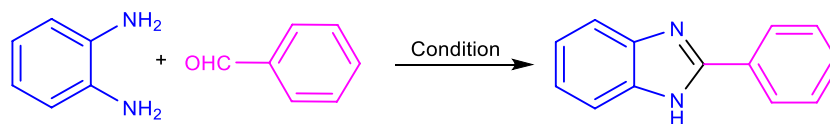
scanning electron microscopy (Fig. 4a). The SEM image shows $\text{CoFe}_2\text{O}_4@\text{SiO}_2@\text{PAF-IL}$ particles are nearly spherical shapes with a mean diameter of 25 nm. The electron-dispersive X-ray spectrum (EDS) confirms the presence of carbon (C), silicon (Si), nitrogen (N), oxygen (O), cobalt (Co), iron (Fe), and iodine (I) elements in $\text{CoFe}_2\text{O}_4@\text{SiO}_2@\text{PAF-IL}$ nanostructure (Fig. 4b). The higher intensity of the Si peak compared to the Fe and Co peaks exhibits the CoFe_2O_4 nanoparticles have been trapped by the SiO_2 layer. So, based on the results, the $\text{CoFe}_2\text{O}_4@\text{SiO}_2@\text{PAF-IL}$ nano-composite has been fabricated successfully.

The magnetic properties for CoFe_2O_4 (a) and $\text{CoFe}_2\text{O}_4@\text{SiO}_2@\text{PAF-IL}$ (b) nanoparticles are measured by vibrating sample magnetometer (VSM) in $-12,000$ to $12,000$ Oe range at room temperature (Fig. 5). The hysteresis loops show superparamagnetic behavior in two samples, and no hysteresis phenomenon was observed. The obtained saturation magnetizations (M_s) for CoFe_2O_4 and $\text{CoFe}_2\text{O}_4@\text{SiO}_2@\text{PAF-IL}$ were observed at 47 and 25 Oe, respectively. These results show that functionalization led to a decrease in the magnetic properties of the nanostructure.

Fig. 5 VSM analysis of CoFe_2O_4 (a) and $\text{CoFe}_2\text{O}_4@\text{SiO}_2@\text{PAF-IL}$ (b)



Scheme 2 The synthesis of 2-arylbenzimidazole and 2-arylbenzothiazole derivatives in the presence of $\text{CoFe}_2\text{O}_4@\text{SiO}_2@\text{PAF-IL}$ as a catalyst

Table 1 The optimization of reaction conditions for synthesis of benzimidazoles and benzothiazoles

Entry	Amount of catalyst (mg)	Temperature (°C)	Solvent	Time (min)	Yield (%)
1	CoFe ₂ O ₄ @SiO ₂ @PAF-IL (10)	Reflux	EtOH	75	70
2	CoFe ₂ O ₄ @SiO ₂ @PAF-IL (10)	Reflux	EtOH: H ₂ O (1:1)	75	65
3	CoFe ₂ O ₄ @SiO ₂ @PAF-IL (10)	Reflux	DMF	75	57
4	CoFe ₂ O ₄ @SiO ₂ @PAF-IL (10)	50 °C	Solvent-free	15	85
5	CoFe ₂ O ₄ @SiO ₂ @PAF-IL (5)	50 °C	Solvent-free	25	77
6	CoFe ₂ O ₄ @SiO ₂ @PAF-IL (20)	50 °C	Solvent-free	15	85
7	CoFe ₂ O ₄ @SiO ₂ @PAF-IL (20)	70 °C	Solvent-free	10	93
8	CoFe ₂ O ₄ @SiO ₂ @PAF-IL (20)	r.t	Solvent-free	60	53
9	CoFe ₂ O ₄ @SiO ₂ @PAF-IL (20)	100 °C	Solvent-free	8	83
10	CoFe ₂ O ₄ (20)	70 °C	Solvent-free	8	80
11	CoFe ₂ O ₄ @SiO ₂ (20)	70 °C	Solvent-free	8	75
12	CoFe ₂ O ₄ @SiO ₂ -PrNH ₂ (20)	70 °C	Solvent-free	8	55
13	CoFe ₂ O ₄ @SiO ₂ @PAF (20)	70 °C	Solvent-free	8	50

Concerning the reaction time and yield of the product, the best results were achieved using Fe₃O₄@SiO₂@PAF-IL as the catalyst (Table 1, entry 7, 10–13).

After optimization of the reaction condition, to determine the generality and efficacy of the hybrid nanocatalyst, various aldehydes carrying either electron-donating or electron-withdrawing groups were reacted under the optimized reaction condition (Scheme 2). It was found that the reactions for all of the various substrates proceed efficiently to produce corresponding 2-arylbenzimidazole and 2-arylbenzothiazole derivatives in good to excellent yields without the formation of side products (Table 2). The aryl aldehydes with electron-withdrawing substituents produced higher yields of desired products compared to aryl aldehydes bearing electron-donating substituents (Table 2). The comparison of CoFe₂O₄@SiO₂@PAF-IL catalyst with some previously reported catalysts for the synthesis of benzimidazole derivatives is shown in Table 3. The presented data confirm that the CoFe₂O₄@SiO₂@PAF-IL is a suitable and efficient catalyst for the synthesis of desired benzimidazole derivatives.

The recovery and reusability of the catalyst are very important for commercial and industrial applications as well as green process aspects. Thus, the recovery and reusability of CoFe₂O₄@SiO₂@PAF-IL was investigated in the model reaction (Fig. 6). After completion of the reaction, the resulting solidified mixture was diluted with hot EtOH (15 mL). Then, the catalyst was easily separated, washed with hot EtOH, dried under vacuum, and reused in a subsequent reaction. Nearly, quantitative recovery of catalyst (up to 96%) could be obtained from each run. As seen in Fig. 6,

the recycled catalyst could be reused six times without any additional treatment or appreciable reduction in catalytic activity. In Fig. 6B and 6C, the FT-IR spectra and XRD patterns of the fresh (a) and reused (b) catalyst are compared, respectively. The consistent structure and activity of recovered and reused CoFe₂O₄@SiO₂@PAF-IL catalyst confirm its stability, recyclability, and performance for the synthesis of desired heterocycles.

Based on the literature survey, two plausible mechanisms for the synthesis of 2-arylbenzimidazole derivatives in the presence of CoFe₂O₄@SiO₂@PAF-IL are depicted in Scheme 3. It is supposed that the reaction proceeds via carbonyl group activation by the hybrid catalyst and subsequent condensation with benzene-1,2-diamine (**1**), leading to the imine intermediate (**I**). In route **A**, the intermediate **I** undergoes ring closure by nucleophilic attack of the second amino group on the imine double bond to gain the intermediate **II**. In the last step, previous studies have proposed aerobic auto-oxidation and aromatization for the conversion of intermediate (**II**) to its corresponding 2-aryl benzimidazoles in the presence of a hybrid catalyst [51, 52]. In route **B**, the intermediate (**II**) is produced via intramolecular cyclization and proton exchange of imine intermediate (**I**). Finally, intermediate (**II**) was transformed into 2-aryl benzimidazoles (**3**) via feasible anomeric-based oxidation (ABO) [40, 53–56]. The major reason for ABO is the driving force of aromatization which will be supported via stereoelectronic and/or anomeric effect [54, 56]. As described, in the ABO process, the C–H bond is so weakened via electron donation from the nitrogen's lone pairs into the C–H anti-bonding orbital

Table 2 Synthesis of benzimidazole and benzothiazole derivatives using $\text{CoFe}_2\text{O}_4@\text{SiO}_2@\text{PAF-IL}$ as a catalyst^a

Entry	Ar	1 or 2	Product	Yield (%)	M.p. (°C)	
					Found	Reported [34–40]
1	C_6H_5	1	4a	93	290–293	290–292
2	4- CH_3 - C_6H_4	1	4b	90	269–271	275–276
3	4- OCH_3 - C_6H_4	1	4c	89	226–227	224–226
4	2-pyridyl	1	4d	87	273–275	271–273
5	2-thiophine	1	4e	80	274–275	274–276
5	4-F- C_6H_4	1	4f	87	223–224	221–224
7	4- NO_2 - C_6H_4	1	4g	94	>300	318–320
8	4-Cl- C_6H_4	1	4h	93	291–292	288–290
9	4-OH- C_6H_4	1	4i	88	265–267	264–265
10	3- OCH_3 -4-OH- C_6H_3	1	4k	90	>300	–
11	4-($\text{N}(\text{CH}_3)_2$)- C_6H_4	1	4l	87	274–277	275–278
12	C_6H_5	2	5a	87	105–107	113–115
13	4- CH_3 - C_6H_4	2	5b	90	84–85	88–89
14	4- OCH_3 - C_6H_4	2	5c	85	120–121	120–121
15	2-pyridyl	2	5d	83	269–271	275–278
16	4-F- C_6H_4	2	5e	90	230–232	231–233
17	4- NO_2 - C_6H_4	2	5f	90	253–255	261–262
18	4-Cl- C_6H_4	2	5g	91	140–142	144–146
19	4-OH- C_6H_4	2	5h	83	221–223	225–227
20	4-($\text{N}(\text{CH}_3)_2$)- C_6H_4	2	5i	83	284–286	284–286

^aReaction condition: benzene-1,2-diamine (**1**, 1 mmol) or 2-aminobenzenethiol (**2**, 1 mmol), Aryl aldehyde (**3**, 1 mmol), $\text{CoFe}_2\text{O}_4@\text{SiO}_2@\text{PAF-IL}$ (20 mg), solvent-free, 70 °C, 10 min

^bIsolated yield

^cThe melting points are not corrected

Table 3 The comparison of $\text{CoFe}_2\text{O}_4@\text{SiO}_2@\text{PAF-IL}$ as a catalyst in the synthesis of benzimidazoles with some other reported catalysts

Entry	Catalyst	Condition	Time (min)	Yield (%)
1	[Dsim]Cl/FeCl ₃	EtOAc, 60 °C	13	93 [35]
2	Co-doped NiFe ₂ O ₄	Solvent-free, 70 °C	55	97 [38]
3	NiEuFe ₂ O ₄	H ₂ O, ultrasonic irradiation	50	84 [37]
4	NH ₃ (CH ₂) ₅ NH ₃ BiCl ₅	Solvent-free, r.t.	6	90 [40]
5	MnFe ₂ O ₄	CH ₃ OH, r.t.	240	92 [51]
6	Cu-complex-phen/bipy-MCM-41	60 °C, ultrasonic irradiation	90	93 [42]
7	[2,6-DMPy-NO ₂]C(NO ₂) ₃	Solvent-free, r.t.	15	95 [54]
8	H ₂ O ₂ , HCl	CH ₃ CN, r.t.	35	97 [57]
9	H ₂ O ₂ , CAN	Solvent-free, 50 °C	35	95 [58]
10	$\text{CoFe}_2\text{O}_4@\text{SiO}_2@\text{PAF-IL}$	Solvent-free, 70 °C	10	93 [This work]

($\sigma^*_{\text{C-H}}$) which can be abstracted via reaction at the surface of the catalyst, to afford molecular hydrogen [54].

Conclusion

In this work, a layer of poly aniline-formaldehyde was fabricated on magnetic nanoparticles surfaces and functionalized by ionic liquid tags successfully. The novel ionic liquid-supported inorganic-polymer hybrid nanostructure

($\text{CoFe}_2\text{O}_4@\text{SiO}_2@\text{PAF-IL}$) was characterized successfully, and its catalytic activity was evaluated in the synthesis of 2-arylbenzimidazole and 2-arylbenzothiazole derivatives. The desired products were synthesized in high yields via feasible anomeric-based oxidation within short reaction times. This protocol has some advantages in terms of solvent-free condition, high yield and purity, easy work-up and eco-friendly process, simple separation of catalyst as well as the recyclability of it without a notable decrease in catalytic performance.

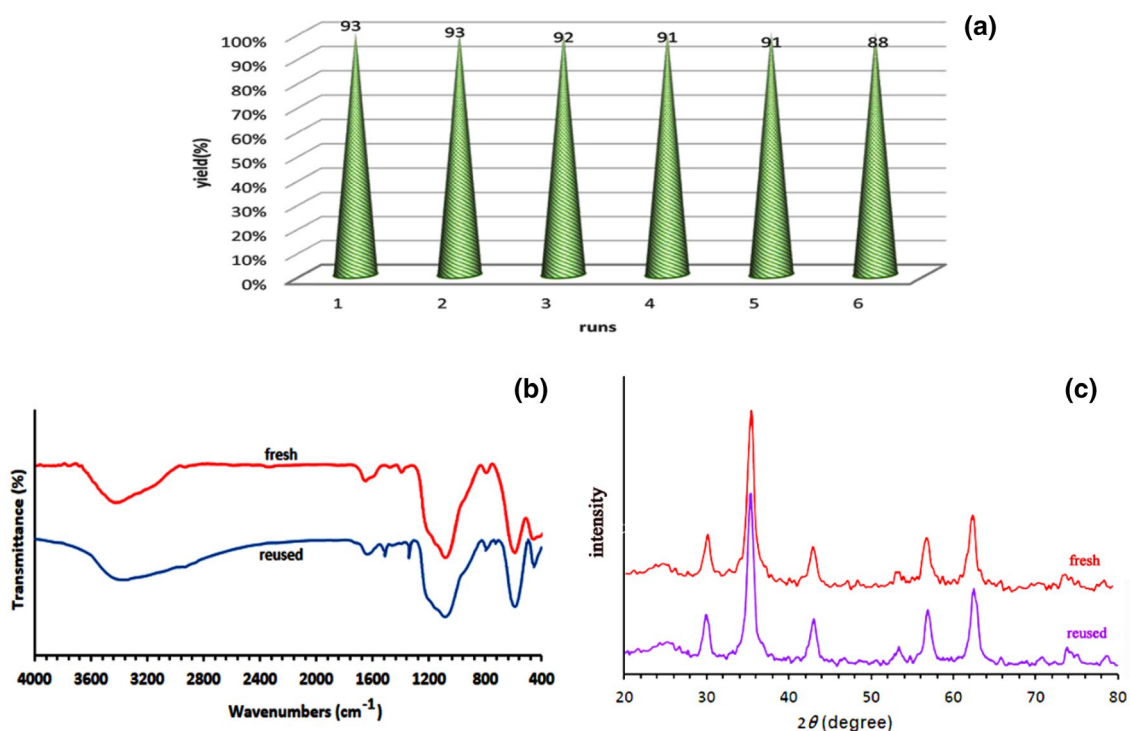
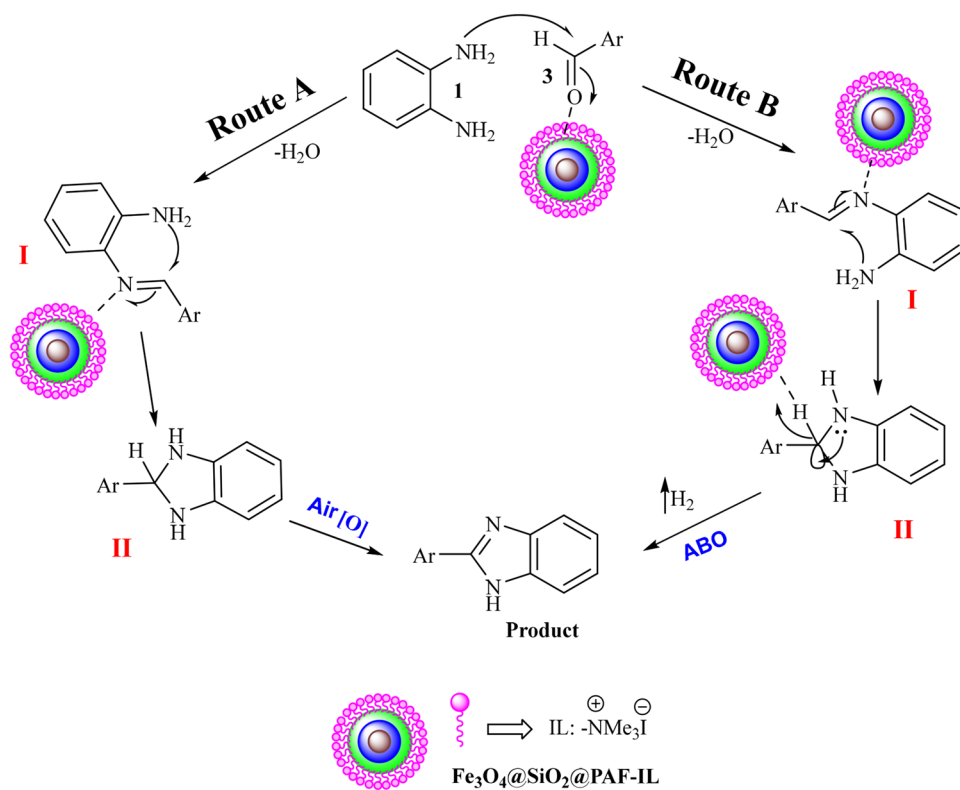


Fig. 6 **a** The recyclability of hybrid nanocatalyst in the model reaction during six runs, **b** FT-IR spectrum, and **c** XRD patterns for fresh and reused catalyst

Scheme 3 The proposed paths for the synthesis of 2-arylbenzimidazole derivatives using $\text{CoFe}_2\text{O}_4@SiO_2@PAF-IL$ as a hybrid catalyst



Acknowledgments The authors acknowledge the financial support (Grant No. 96/2344) of the research council of Arak University.

References

- V.I. Pârvulescu, C. Hardacre, *Chem. Rev.* **107**, 2615–2665 (2007)
- N. Taheri, F. Heidarizadeh, A. Kiasat, *J. Magn. Magn. Mater.* **428**, 481–487 (2017)
- R. Vekariya, *J. Mol. Liq.* **227**, 44–60 (2017)
- M. Vafaezadeh, Z. Bahrami Dizicheh, M. Mahmoodi Hashemi, *Catal. Commun.*, **41**, 96–100 (2013)
- S.K. Singh, A.W. Savoy, *J. Mol. Liq.* **297**, 112038 (2020)
- M.A. Bodaghifard, M. Hamidinasab, N. Ahadi, *Curr. Org. Chem.* **22**, 234–267 (2018)
- H. Li, P.S. Bhadury, B. Song, S. Yang, *RSC Adv.* **2**, 12525–12551 (2012)
- W. Xie, F. Wan, *Chem. Eng. J.* **365**, 40–50 (2019)
- M. Przepis, K. Matuszek, A. Chrobok, M. Swadźba-Kwaśny, D. Gillner, *J. Mol. Liq.* **308**, 113166 (2020)
- Z. He, D. Liu, Z. Zhou, P. Wang, *J. Sep. Sci.* **36**, 3226–3233 (2013)
- H. Sahebi, E. Kono, A. Ezabadi, *New J. Chem.* **43**, 13554–13570 (2019)
- J. Fu, H. Zang, Y. Wang, S. Li, T. Chen, X. Liu, *Ind. Eng. Chem. Res.* **51**, 6377–6386 (2012)
- W. Injumba, P. Ritprajak, N. Insin, *J. Magn. Magn. Mater.* **427**, 60–66 (2017)
- V. Polshettiwar, B. Baruwati, R. S. Varma, *Chem. Comm.*, 1837–1839 (2009)
- F. Shi, M.K. Tse, M.M. Pohl, A. Brückner, S. Zhang, M. Beller, *Ang. Chem. Int. Ed.* **46**, 8866–8868 (2007)
- T.W. Prow, J.E. Grice, L.L. Lin, R. Faye, M. Butler, W. Becker, E.M.T. Wurm, C. Yoong, T.A. Robertson, H.P. Soyer, M.S. Roberts, *Adv. Drug Deliv. Rev.* **63**, 470–491 (2011)
- A. Farzin, S.A. Etesami, J. Quint, A. Memic, A. Tamayol, *Adv. Healthc. Mater.* **9**, 1901058 (2020)
- Q. Chaudhry, L. Castle, *Trends Food Sci. Tech.* **22**, 595–603 (2011)
- R. Nair, S.H. Varghese, B.G. Nair, T. Maekawa, Y. Yoshida, D.S. Kumar, *Plant Sci.* **179**, 154–163 (2010)
- F.M. Kelly, J.H. Johnston, A.C.S. Appl. Mater. Inter. **3**, 1083–1092 (2011)
- T.A. Dankovich, D.G. Gray, *Environ. Sci. Technol.* **45**, 1992–1998 (2011)
- G.V. Jacintho, A.G. Brolo, P. Corio, P.A. Suarez, J.C. Rubim, *J. Phys. Chem. C* **113**, 7684–7691 (2009)
- X. Ren, J. Shi, L. Tong, Q. Li, H. Yang, *J. Nanopart. Res.* **15**, 1738 (2013)
- Z. Mahhouti, H. El Moussaoui, T. Mahfoud, M. Hamedoun, M. El Marssi, A. Lahmar, A. El Kenz, A. Benyoussef, *J. Mater. Sci.: Mater. Electron.* **30**, 14913–14922 (2019)
- A. Ivanković, A. Dronjić, A.M. Bevanda, S. Talić, *Int. J. Sustain. Green Energ.* **6**, 39–48 (2017)
- A. Valavanidis, T. Vlachogianni, K. Fiotakis, International Conference “Green Chemistry and Sustainable development”, Thessaloniki, 25–26 (2009)
- S. Tahlan, S. Kumar, B. Narasimhan, *BMC Chem.* **13**, 18 (2019)
- S.A. El-Feky, H.K. Thabet, M.T. Ubeid, *J. Fluori. Chem.* **161**, 87–94 (2014)
- I. Yildiz-Oren, I. Yalcin, E. Aki-Sener, N. Ucarturk, *Europ. J. Med. Chem.* **39**, 291–298 (2004)
- D. Kumar, M.R. Jacob, M.B. Reynolds, S.M. Kerwin, *Bioorg. Med. Chem.* **10**, 3997–4004 (2002)
- C.W. Evans, C. Atkins, A. Pathak, B.E. Gilbert, J.W. Noah, *Antiv. Res.* **121**, 31–38 (2015)
- N. Kaur, A. Kaur, Y. Bansal, D.I. Shah, G. Bansal, M. Singh, *Bioorg. Med. Chem.* **16**, 10210–10215 (2008)
- N. Siddiqui, S.N. Pandeya, S.A. Khan, J. Stables, A. Rana, M. Alam, M.F. Arshad, M.A. Bhat, *Bioorg. Med. Chem. Lett.* **17**, 255–259 (2007)
- G.R. Bardajee, M. Mohammadi, H. Yari, A. Ghaedi, *Chin. Chem. Lett.* **27**, 265–270 (2016)
- A. Khazaei, M.A. Zolfigol, A.R. Moosavi-Zare, A. Zare, E. Ghaemi, V. Khakyzadeh, Zh. Asgari, A. Hasaninejad, *Sci. Iran.* **18**, 1365–1371 (2011)
- Y. Merroun, S. Chehab, T. Ghailane, M. Akhazzane, A. Souizi, R. Ghailane, *React. Kinet. Mech. Catal.* **126**, 249–264 (2019)
- A. Ziarati, A. Sobhani-Nasab, M. Rahimi-Nasrabadi, M.R. Ganjali, A. Badiei, *J. Rare Earths* **35**, 374–381 (2017)
- A. Karimian, R. Mohammadzadeh Kakhki, H. Kargar Beidokhti, *J. Chin. Chem. Soc.*, **64**, 1316–1325 (2017)
- L.Z. Fekri, M. Nikpassand, R. Maleki, *J. Mol. Liq.* **222**, 77–81 (2016)
- Z. Benzekri, S. Sibous, H. Serrar, A. Ouasri, S. Boukhris, A. Rhandour, A. Souizi, *J. Iran. Chem. Soc.* **15**, 2781–2787 (2018)
- N. Foroughifar, A. Mobinikhaledi, S. Ebrahimi, M.A. Bodaghifard, H. Moghanian, *J. Chin. Chem. Soc.* **56**, 1043–1047 (2009)
- A. Mobinikhaledi, M. Zendehtdel, M. Hamidinasab, M.A. Bodaghifard, *Heterocycl. Commun.* **15**, 451–458 (2009)
- M.A. Bodaghifard, A. Mobinikhaledi, M. Hamidinasab, *Synth. React. Inorg. Met.-Org. Nano-Metal. Chem.* **44**, 567–571 (2014)
- M.A. Bodaghifard, Z. Faraki, A.R. Karimi, *Curr. Org. Chem.* **20**, 1648–1654 (2016)
- M.A. Bodaghifard, A. Mobinikhaledi, S. Asadbegi, *Appl. Organomet. Chem.* **31**, e3557 (2017)
- M. Zendehtdel, M.A. Bodaghifard, H. Behyar, Z. Mortezaei, *Micropor. Mesopor. Mat.* **266**, 83–89 (2018)
- H. Moghanian, M.A. Bodaghifard, A. Mobinikhaledi, N. Ahadi, *Res. Chem. Intermed.* **44**, 4083–4101 (2018)
- N. Ahadi, M.A. Bodaghifard, A. Mobinikhaledi, *Appl. Organomet. Chem.* **33**, e4738 (2019)
- D. Moitra, S. Hazra, B.K. Ghosh, R. Jani, M. Patra, S.R. Vadera, N.N. Ghosh, *RSC Adv.* **5**, 51130–51134 (2015)
- J. Yamuna, T. Siva, S. S. Sreeja Kumari, S. Sathiyarayanan, *RSC Adv.* **6**, 79–86 (2016)
- G. Brahmachari, S. Laskar, P. Barik, *RSC Adv.* **3**, 14245–14253 (2013)
- M. Bharathi, S. Indira, G. Vinoth, T. Mahalakshmi, E. Induja, K. Shamuga Bharathi, *J. Coord. Chem.*, **73**, 653–670 (2020)
- M.A. Zolfigol, M. Safaiee, B. Ebrahimghasri, S. Baghery, S. Alaie, M. Kiafar, A. Taherpour, Y. Bayat, A. Asgari, *J. Iran. Chem. Soc.* **14**, 1839–1852 (2017)
- M.A. Zolfigol, A. Khazaei, S. Alaie, S. Baghery, F. Maleki, Y. Bayat, A. Asgari, *RSC Adv.* **6**, 58667–58679 (2016)
- P. Ghasemi, M. Yarie, M.A. Zolfigol, A. Taherpour, M. Torabi, *ACS Omega* **5**, 3207–3217 (2020)
- Meysam Yarie, *Iran. J. Catal.* **10**, 79–83 (2020)
- K. Bahrami, M. M. Khodaei, I. Kavianinia, *Synthesis*, 547–550 (2007)
- K. Bahrami, M.M. Khodaei, F. Naali, *J. Org. Chem.* **73**, 6835–6837 (2008)